Investigation of the dynamic SPECT (dSPECT) method for Teboroxime using a 4-D kinetic thorax model dMCAT

A. Celler[†], S.Blinder[†], D. Noll[‡], T.Tyler[§], F.Duclercq[‡], R. Harrop[†]
[†]Div. of Nuclear Medicine, Vancouver Hospital and Health Sciences Centre, Vancouver, B.C., Canada
[‡]Mathématiques pour l'Industrie et la Physique (MIP), Université Paul Sabatier, Toulouse, France
[§]Department of Engineering Physics, Simon Fraser University, Burnaby, B.C., Canada

Abstract

Tomographic SPECT allows us to visualize, in 3D, the distribution of radiopharmaceuticals in the body which are reconstructed from a series of two dimensional measurements performed around the investigated object. The dSPECT method extends these capabilities into the fourth dimension and creates a series of dynamic 3D images which can be obtained from a single set of dynamic data acquired using only a single rotation of the camera. In order to test the performance of the method for Teboroxime cardiac images, we have modified the 3D MCAT digital phantom to model dynamic changes of activity distributions in different organs of the thorax. Experiments using different acquisition protocols were performed and the resulting data were reconstructed using static (FBP and OSEM) and dynamic (dEM) methods. The images obtained by summing the data from dynamic reconstructions over all time-frames were as good as or better than those from static reconstructions (for the scans which begun 60 or 120 seconds post injection i.e. after the bolus of activity left the heart). Including the bolus in the reconstructions produced distorted images. An important advantage of the dSPECT method is that it reconstructs images in a form of 3D movies that may be used to extract additional diagnostic information, mainly temporal information which is not available in static images and 3D spatial information not present in planar studies.

I. Introduction

Single Photon Emission Computed Tomography (SPECT) is well recognized as a powerful diagnostic tool to investigate organ function rather than anatomy since it allows us to image, in three dimensions, the bio-distribution of radiolabelled tracers within the body. Standard clinical SPECT methods, however, image only stationary activity distributions. It is believed that nuclear medicine procedures which could trace changing distributions of radio-labelled substances would provide important information for both diagnosis and research (see for example [1, 2]).

To this end we have proposed a dynamic SPECT (dSPECT) method [3] that allows us to obtain quantitative information about kinetic processes in the body from the data acquired using a standard clinical acquisition protocol, one with a single rotation of a tomographic camera. The method can be used with all standard, currently available SPECT systems including single, double and triple head cameras. The result of the dSPECT reconstruction, which includes attenuation and resolution recovery corrections, is a 4D data set, composed of a time-series of 3-D SPECT images (3D movie). The dSPECT reconstruction is based on a mathematical optimization procedure where all the dynamic projections are being considered simultaneously, resulting in images with better signal to noise ratio than in the "fast-rotation" method, where each data set is reconstructed separately. An important feature of the method is that each dynamic voxel (doxel) is reconstructed independently and, as a result, it is possible for an object to contain an assortment of doxels where the activity may increase, decrease, increase and decrease or remain constant over the acquisition time.

Over the last few years we have investigated the performance of the method using 2D computer simulations, phantom experiments and patient studies [3, 4, 5]. The goal of these tests has been to verify the method for a broad range of kinetic parameters, to evaluate its accuracy and to optimize acquisition protocols. At the present stage, however, we are focusing our research on a few practical applications of the method. One of such applications is investigation of cardiac studies using Teboroxime Tc-99m.

It has been shown that Teboroxime extraction reflects the true blood flow better than other myocardial perfusion agents such as Tc-99m MIBI or Tl-201 [6, 7]. Its use has been limited because it is not trapped within the cell, but rather, due to its neutral charge, is rapidly washed out. Thus, using standard static imaging methods with this radiopharmaceutical is difficult. Image artifacts can be produced and also, as will be shown later in this paper, the location, or even the presence of any defect can often not be visualized due to the delay of blood perfusion in the stenotic area.

In order to investigate these issues we have adapted the 3D mathematical cardiac torso phantom (MCAT) [8] to model temporal changes in activity distributions. Using a dynamic version of the model (dMCAT) we have simulated different clinical situations and acquisition protocols, then assessed the diagnostic content of images obtained from this data using static and dynamic reconstructions. Although in this work we present only the results of Teboroxime simulations, the dMCAT phantom is fully versatile and can be used with other radiopharmaceuticals using appropriate compartmental models.

II. Methods

In our dynamic version of the model (dMCAT) we first simulate the time-activity concentrations of the radiotracer in different organs of the human thorax using a compartmental

model approach. A set of differential equations representing the flow of activity between organs is solved with kinetic parameters being defined by the user in a MATLAB user interface. This part of the program has to be modified for each tracer so that the equations match the appropriate compartmental model. The result of this calculation is displayed on a graph as a set of time activity curves (TAC) representing concentrations in different compartments. In our simulations these activity changes were modeled assuming a bolus injection of the tracer. The activity then moves from the right ventricle to the lungs, next to the left ventricle, and to the myocardium, the muscles (representing the rest of the body) and to the liver. An additional equation is used to create a defect in the heart with dynamic parameters different from those of a healthy myocardium. Kinetic parameters used in the model were based on experimental Teboroxime studies and the shapes of the resulting simulated TAC's were adjusted to match the experimental shapes [9, 10]. Figure 1 shows an example of the curves used in our simulations. As can be seen from this figure, the injection bolus lasts for about 30 seconds in the right ventricle, then, for the next 30-60 seconds the activity in all organs rises fast and this period is followed by much slower changes, with the normal myocardium washout characteristic time in the range of 6-8minutes.

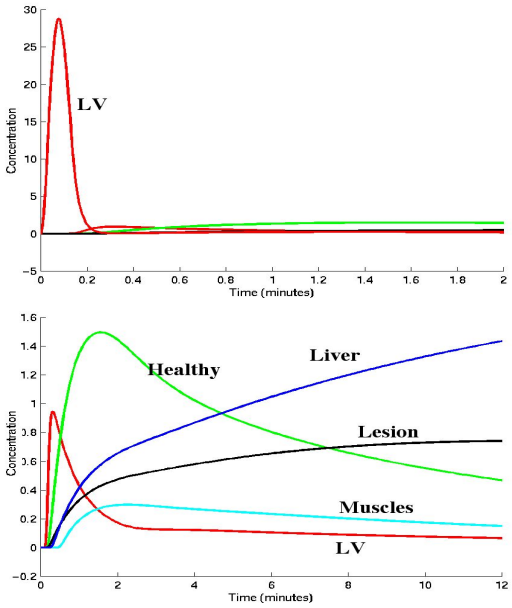

Figure 1: An example of the time activity curves (TAC) used in Teboroxime dMCAT simulations. The top part of the figure shows the injection bolus as it moves through the right ventricle and the lower part the activity concentrations in the remaining. Note the change of scale between the images.

In the next step these values of activity concentration are used to compute the 4D thorax model (the "truth") with the activity in each organ following a separate time activity change. Figure 2 shows a volume rendered image of the dMCAT with activities corresponding to 2 minutes post injection. We have simulated the healthy myocardium and the one with stenosis (heart defect) located at two different places in the heart (in the apex and close to the liver). Also, two different levels of

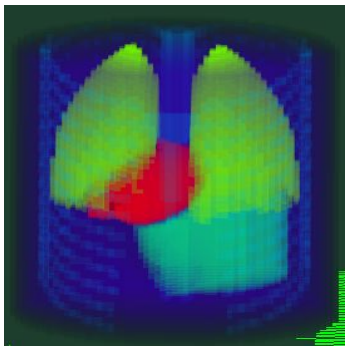

Figure 2: A volume rendered image of the dMCAT phantom with activities in the organs corresponding to 120 seconds (2 minutes) post injection.

liver uptake were modeled with the MCAT option of a liver positioned high in the thorax.

The user then specifies the acquisition parameters using a MATLAB user interface. The number of camera heads, their starting angle, the matrix and pixel sizes, the angle of rotation, the time of each camera stop and the time between the injection and the beginning of the acquisition are specified to generate the projector without or with attenuation and without or with 2D or 3D collimator blurring. At this point the sinograms are calculated.

In our tests we have investigated all these options modeling slow acquisitions with dual and triple head systems, rotating a maximum 180° per head. In all cases the matrix size was 64 x 64 with 64 or 32 camera stops and 10 or 20 seconds per projection, respectively. Two different approaches were tested: (i) a short 3 minute scan where the activity in the object does not change too much and (ii) a longer 10 minute scan during which the activity drops by about 50%, this allows us to collect dynamic data with better statistics and with more data points. Similarly, we have tested acquisitions starting (a) at the time of injection (at 0 seconds) where fast movement of bolus through the heart is strongly influencing the projection data, (b) at 60 seconds post injection with more moderate rates of change and the with increase and decrease of activity in the organs, and (c) at 120 seconds post injection where activity changes are the slowest.

Noiseless as well as noisy projection data (according to a Poisson noise) corresponding to about 7-8 counts per second per milliliter of myocardium tissue as measured at 120 seconds post injection (based on real patient data) were created. Additionally, an experiment simulating triple-head fast rotation was performed with the camera rotating for 20 seconds over 120° per head. This study was started at 60s post injection and continued for 10 minutes (30 rotations in total).

The last part of our MATLAB interface allows us to reconstruct the data using (i) static reconstruction methods: filtered backprojection (FBP) or ordered subsets expectation maximization (OSEM) or (ii) using a dynamic approach with 2D [11] or 3D [12] dynamic expectation maximization (dEM) reconstructions. All images presented in this work were smoothed using a 3x3 gaussian filter.

III. Results and Discussion

First, in order to check the results for the presence of artifacts, the static reconstructions were compared with the images obtained by summing dynamic images over all time frames. The static images obtained from the data from both acquisitions which started at the moment of injection (0-3 minutes and 0-10 minutes) were dominated by strong streak artifacts which were due to large variations in the object created by the bolus activity entering the right and later the left ventricle. As expected, the FBP images were much worse than those from the OSEM method. Dynamic reconstructions, which have the advantage of creating a whole time-series of images, displayed some artifacts in the first images corresponding to the beginning of the scan, but were surprisingly good for the remaining time frames. These results indicate that dSPECT can handle even large activity changes. Summing of the time frames in this case did not make much sense, as artifacts from these first frames dominated and spoiled the resulting images as it is illustrated on Figure 4.

Similar comparisons were performed for scans starting at 60 and 120 seconds post injection. In this case, although FBP static images were bad, the OSEM and summed over time dEM reconstructions produced very comparable images (see Figure 4). Also, there was not much difference between the acquisitions which started at 60 and 120 seconds post injection. Careful analysis of this data, however, reveals one disturbing effect. Both static and summed dynamic reconstructions tend to average the activity distributions over time. Therefore, in situations where there is a defect in the heart it is possible that both normal and stenotic myocardium will have equal levels of such an averaged activity and therefore these images will not reveal the location, or even the presence, of the defect. On the other hand, when reviewing the dynamic time series reconstructed using the dSPECT method one can clearly identify the defect and analyse its perfusion. Figure 5 presents two dynamic times-frames (80 and 260 seconds) corresponding to the same data as presented in Figure 4. Changes in relative levels of activity display clearly the location of the defect. For comparison, the top two images present the true activity distributions, in the middle the results of dSPECT reconstruction are displayed and the bottom part presents images obtained using the data acquired with the fast rotation of the triple head camera reconstructed with OSEM. Since these images correspond to only 20 seconds total acquisition time they have very poor statistics and the high noise makes their analysis practically impossible.

On the other hand, when reviewing the dSPECT reconstruction, in addition to spatial information about the activity distribution, a dynamic series of images also contains temporal information which can be used in subsequent analysis for diagnostic purposes or in order to separate different organs. Important applications of this approach would be the identification and quantitation of heart defects and the elimination of the problem of overlapping liver and heart distributions. The time activity curves for normal and diseased

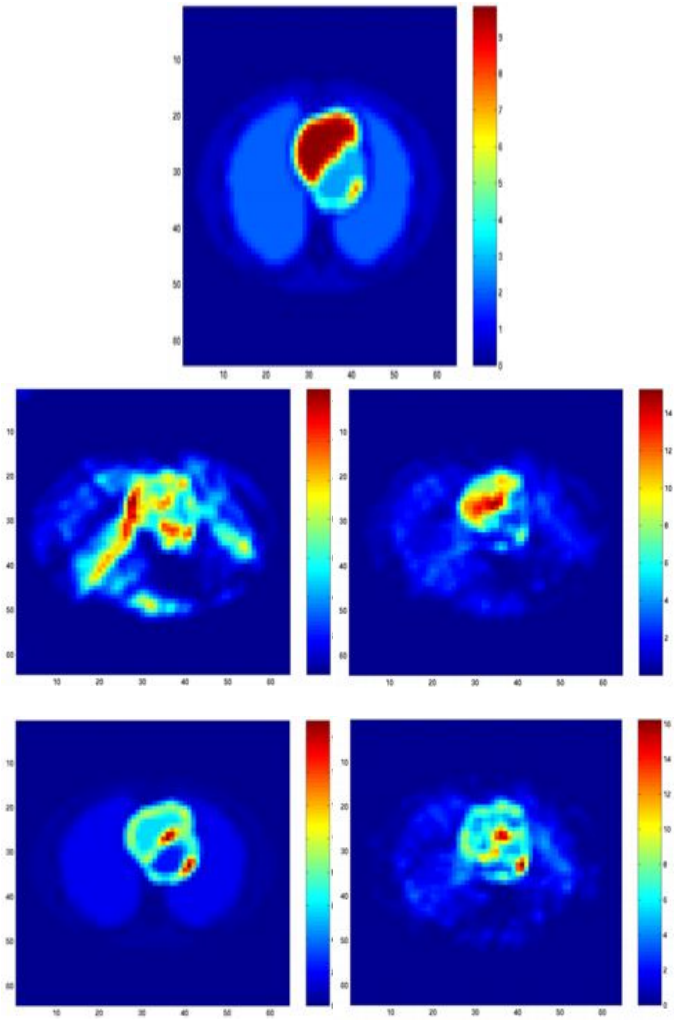

Figure 3: Images of a transaxial slice of the dMCAT phantom for 3 minutes acquisitions starting at the time of the injection. The true activity distribution (upper) and the results of static OSEM (middle left), and dynamic dEM summed over all time frames (middle right) are presented. In the bottom part of the figure the true and the dSPECT images corresponding to the 2.5 minute time frame are displayed.

myocardium and for the liver are quite different (see Figure 1) and, indeed, dynamic data could be used in a such separation procedure.

IV. Conclusions

Performance of the dSPECT method has been investigated for myocardial viability studies with Teboroxime using the MCAT phantom, which was modified to model changing activity distributions in the organs. The images which were obtained by summing the images from dynamic reconstructions over all time-frames were as good and often better or even much better than those from static FBP or OSEM. An important advantage, however, of the dSPECT method is that it reconstructs images in a form of 3-D dynamic movies that may be used to extract additional diagnostic information. All these findings need to be confirmed in patient studies which are currently being performed.

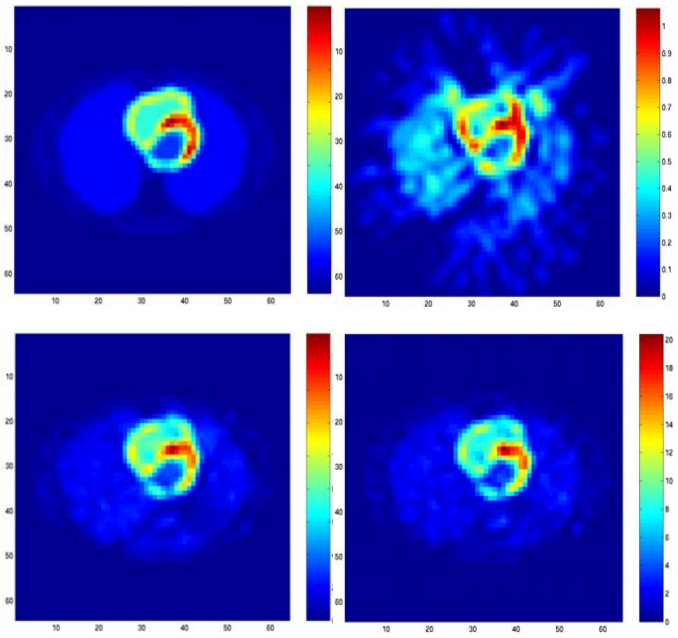

Figure 4: Images of a transaxial slice of the dMCAT phantom. The true activity distribution (upper left) and the results of static FBP (upper right), static OSEM (lower left) and dynamic dEM summed over all time frames (lower right) are presented.

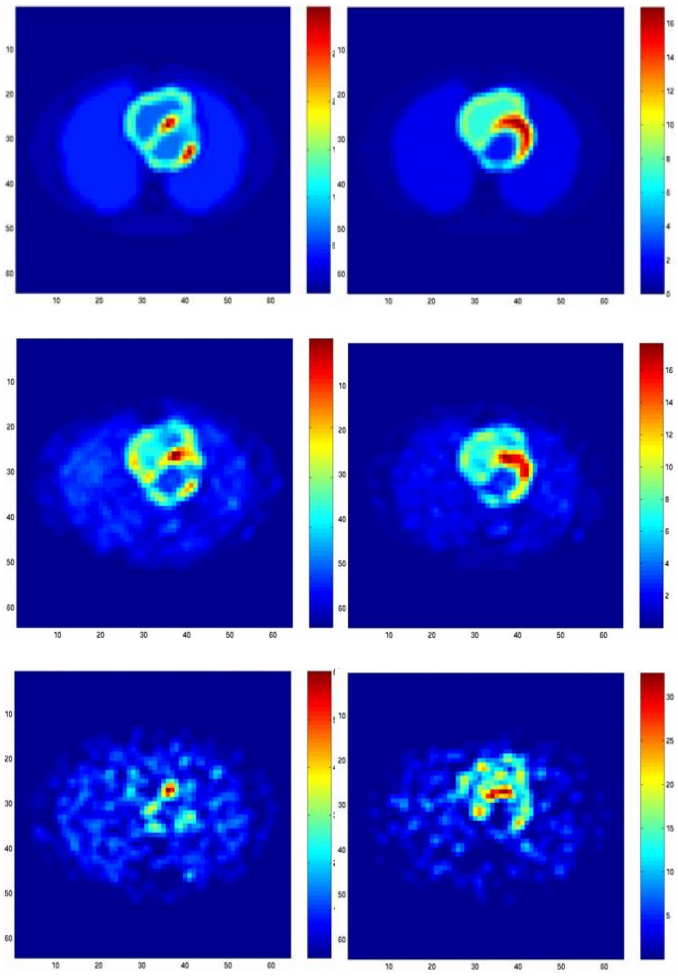

Figure 5: Images of a transaxial slice of the dMCAT phantom corresponding to the activity distribution at 80 seconds (left) and 260 seconds (right). The true activity distribution (upper row), the results of dynamic dEM (middle row), and dynamic "fast-rotation" (bottom row) are presented.

V. References

[1] R. Stewart, B.Heyl, R.O'Rourke, R.Blumhardt, and D. Miller. Demonstration of differential post-stenotic myocardial technetium-99m-teboroxime clearance kinetics after experimental ischemia and hyperemic stress. *J. Nuc. Med.*, 32(10):2000–2008, 1991.

[2] H. Weinstein, S.T. Dahlberg, B.A. McSherry, R.C. Hendel, and J.A.Leppo. Rapid redistribution of teboroxime. *Am. J. Cardiol.*, 71:848–852, April 1999.

[3] T. Farncombe, A. Celler, D. Noll, J. Maeght, and R. Harrop. Dynamic SPECT imaging using a single camera rotation (dSPECT). *IEEE Trans. Nuc. Sci.*, 46(4):1055–1061, 1999.

[4] A.Celler, T.Farncombe, C.Bever, D.Noll, J.Maeght, R.Harrop, and D. Lyster. Performance of the dynamic single photon computed tomography (dspect) method for decreasing or increasing activity changes. *Phys. Med. Biol.*, 45:3525–3544, 2000.

[5] T. Farncombe, A. Celler, D. Noll, J. Maeght, and R. Harrop. The incorporation of organ uptake into dynamic spect (dSPECT) image reconstruction. *IEEE Trans. Nuc. Sci.*, 48(1):3–9, 2001.

[6] R. Narra, A. Nunn, B. Kuczynski, T. Feld, P. Wedeking, and W. Eckelman. A neutral technetium-99m complex for myocardial imaging. *J. Nuc. Med.*, 30:1830–1837, 1989.

[7] Q-S. Li, G. Solot, T.L.Frank, Jr H.N. Wagner, and L.C. Becker. Tomographic myocardial perfusion imaging with technetium-99m-teboroxime at rest and after dipyridamole. *J. Nuc. Med.*, 32(10):1968–1976, 1991.

[8] P.H. Pretorius, M.A. King, B.M.W.Tsui, K.J. LaCroix, and W. Xia. A mathematical model of motion of the heart for use in generating source and attenuation maps for simulating emission imaging. *Med. Phys.*, 26:2323–2332, 1999.

[9] A.M. Smith, G.T. Gullberg, P.E. Christian, and F.L. Datz. Kinetic modeling of teboroxime using dynamic SPECT imaging of a canine model. *J. Nuc. Med.*, 35:484–495, 1994.

[10] A. Sitek, E.V.T. DiBella, and G.T. Gullberg. Factor analysis with a priori knowledge - application in dynamic cardiac spect. *Phys. Med. Biol.*, 45:2619–2638, 2000.

[11] T.Farncombe, S.Blinder, A.Celler, D.Noll, J.Maeght, and R.Harrop. A dynamic expectation maximization algorithm for single camera rotation dynamic spect (dspect). *IEEE Nuclear Science Symposium Conference Record*, 2000.

[12] T.H. Farncombe, M.A. King, A. Celler, and S.Blinder. A fully 4d expectation maximization algorithm using gaussian diffusion based detector response for slow camera rotation dynamic spect. In *Proceedings of the 2001 International Meeting on Fully 3D Image Reconstruction in Radiology and Nuclear Medicine*, 2001. submitted.